Cost Disruptive Reflector Surface for Large Deployable Antennas

Mike Lawton
Oxford Space Systems
Satellite Applications Catapult, Harwell OX11 OQR; 07740937935
mike.lawton@oxfordspacesystems.com

Juan R Reveles
Oxford Space Systems
Satellite Applications Catapult, Harwell OX11 OQR; 07827441738
juan.reveles@oxfordspacesystems.com

Zhong You
University of Oxford
Department of Engineering Science, OX1 3PJ; 01865283301
zhong.you@eng.ox.ac.uk

Ashley Dove-Jay, Amjad Khan, Vincent Fraux
Oxford Space Systems
Satellite Applications Catapult, Harwell OX11 OQR

ABSTRACT

Current flight solutions for Large Deployable Antennas (LDA) most commonly employ the use of highly flexible metal wire knitted meshes as a reflector surface material. These surfaces, also known as 'tricot meshes', are normally realized using gold plated molybdenum and tungsten wires and require tensioning in the range of 5-10g/cm to obtain sufficient electrical contact between wires and to reduce surface RMS deformation to an acceptable level. The cell or facet size of a knitted mesh is determined by the operating frequency; the higher the frequency the higher the cell density required. Meshes are well known for lower frequency (L and S-band) applications but the challenges of operating LDAs at desired higher frequencies (Ka-band) means metal mesh surfaces require increasingly complex cable tensioning nets and a deviation away from proven mesh materials. High frequency operation of metal meshes also increases the likelihood of Passive Intermodulation (PIM) occurring and thus a degradation in the performance of the antenna.

Due to the increasing difficulties and shortcomings of metal meshes encountered when attempting to operate at ever higher frequencies, Oxford Space Systems (OSS) is developing a flexible reflector surface based upon the use of flexible carbon fibre composite material. Preliminary results suggest the surface material lends itself to being folded in such a manner as to be compatible with the stowage requirements of common LDA architectures. A key property of the material is its ability to be pre-molded and thus it effectively seeks to achieve the shape of its original mold. The result is that, under micro-gravity, the surface will naturally tend toward the desired reflector surface profile thus minimizing the need of surface pre-tensioning. This reduces the need for cable tensioning net systems and thus the design complexity and cost of the reflector surface backing structure.

This paper describes the use of a proprietary outer ring deployment mechanism for the OSS surface material in order to achieve a complete LDA solution. OSS has successfully undertaken the development of a novel, mobility-1 TRL3 Reflector Deployable Structure (RDS) suitable for LDA applications. By overcoming the deficiencies of so called over-constrained mechanisms, OSS will present a cost disruptive, scalable LDA concept targeted at operation at frequencies up to Ka-band. Being mobility-1, the motion structure can be actuated from a single point by means of a novel linear actuator.

KEYWORDS: motion structure, large deployable antenna, foldable reflector, unfurlable reflector

INTRODUCTION

A high maturity European Large Deployable Antenna (LDA) capability in the diameter range of 4 to 9 metres is seen as strategically important[1] due to their wide applicability to broadband satellite telecommunication services.

S. Hatton (ed.), *Proceedings of the 13th Reinventing Space Conference*,
https://doi.org/10.1007/978-3-319-32817-1_10

Currently the LDA market is dominated by US corporate organisations with AstroMesh arguably regarded as the industry state-of-the-art LDA[1]. Developing a European supplier of LDAs to meet the demands of European customers in the first instance is seen as paramount by European industry primes and the European Space Agency (ESA).

The future market requirement for LDAs is expected to be driven by demands from commercial, military and scientific sectors. The commercial demand from fixed & broadcasting satellite services together with multi-media networks requiring satellites as an integral part of network infrastructure represent the greatest demand segment.

In Reference 1, it is reported that customer primary requirements for LDAs are driven by:

- High reliability
- Cost competitive
- Mass efficient
- Maintain high reflector surface integrity
- High stowage efficiency
- Side attachment capability
- Acceptable deployment time

Taking these requirements as their basis for their design, the Oxford Space Systems (OSS) team undertook the development of a novel outer ring mechanism suitable for a Large Deployable Antenna (LDA) capable of supporting both a novel flexible carbon fibre reflector surface as well as a more conventional metal mesh. This led to the realisation of a 4 metre diameter breadboard (BB) demonstrator of the deployable backing structure[4]. The purpose of the breadboard was to validate and demonstrate the kinematics of the chosen concept together with some of the key benefits of the selected deployable ring structure. The concept selected for the structure is an adaptation of the Sarrus mechanism with a pantograph adjusted to maintain a constant angle between the neighbouring vertical bars and therefore maintain a constant pyramid angle. The breadboard structure weighs 7.0kg and deploys from a minimum diameter of 0.23m to 4m. When the structure is stowed, an internal cylindrical volume of 0.18m diameter is achieved to allow the storage of the reflector surface material and supporting cable network. Several tests were conducted on the breadboard to determine the viability of the concept with encouraging results[5].

With regard to the flexible reflector surface materials, OSS' current development approach consists of formulating and manufacturing a range of reflector surface composite coupons from an array of space compatible carbon fibre structures, silicone compounds, and metallic nanoparticle materials. These coupons are tested for their radio frequency (RF) performance in terms of reflection efficiency and transmission losses at Ka-band, under the European Space Agency (ESA) definition of 26.5 – 40 GHz and over a range of temperatures (-180C to +100C). The best performing of these coupons has been taken forward for mechanical testing in the form of minimum bend radius testing to explore the folding feasibility and therefore stowage efficiency capabilities. Using this information, initial finite element (FE) studies into folding configurations and associated bend radii are presented. The preliminary results for the reflector surface are encouraging but it is acknowledged that the current development is still in its infancy and a rigorous qualification campaign is thus required.

DESCRIPTION OF KEY BUILDING BLOCKS OF THE LDA THE TECHNOLOGY

In this section the RDS architecture (the Sarrus-Pantograph based architecture) developed by OSS is described; this concept has been progressed to TLR3 and has undergone basic testing consistent with its technology level. Subsequently, the flexible reflector surface material is described and preliminary performance results presented.

Sarrus-Pantograph Based RDS Architecture

The Sarrus mechanism is a special case of a spatial closed chain in which the Kutzbach criterion for mobility becomes zero (or negative in the case of the Sarrus mechanism with a pantograph element)[3]:

$$m = 6n - 5j - 6 \qquad (1)$$

In Eq. 1, *m* refers to the mechanism mobility; *n* refers to the number of linkages and *j* to the numbers of joints. This holds for a closed chain where only lower pair joints (e.g. revolute, prismatic, screw, cylindrical, spherical or planar joints) are involved and where each joint has one degree of freedom. Evidently, for a spatial closed chain to have mobility 1 (m=1), seven links (n=7) and seven joints (j=7) are needed; any kinematic chain with fewer links and joints is to be either immobile or overconstrained. Immobile structures find no applicability in LDAs for obvious reasons. As for overconstrained mechanisms, they can be traced back to Pierre Frederic Sarrus who in 1853 reported a six bar mechanism capable or rectilinear motion. The OSS architecture is a closed kinematic chain which, following the accepted mobility criterion, can be described as a modified overconstrained 6-bar Sarrus linkage mechanism with 6 one-degree-of-freedom (revolute) joints which displays mobility one.

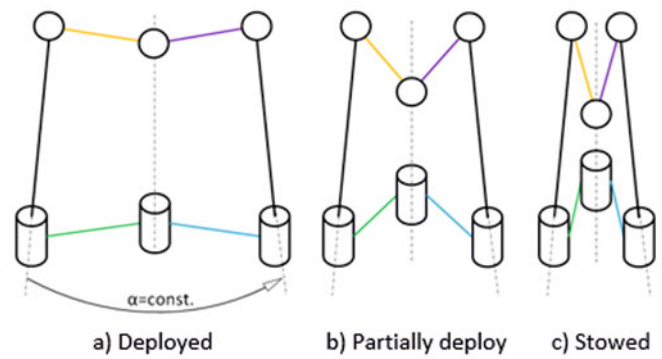

Figure 1 Sarrus linkage schematic diagram

This linkage arrangement allows the chosen angle α between the vertical bars (black bars in Figure 1 above) to remain constant (Figures 1 and 2). This characteristic is also displayed by other deployable structure concepts such as the one developed and patented by ESA[6]. By carefully arranging the facet presented in Figure 1 a hexagonal pyramid of constant angle can be obtained (Figure 3).

The pantograph is introduced into the Pure Sarrus mechanism as a simple means of synchronisation of all the elements of the close kinematic chain.

For the pantograph sliding joints to follow the right path while deploying and maintain a constant angle α between the vertical bars, the following dimensioning rule has to be respected (Figure 2)[3]:

$$l1 = l2 \qquad (2)$$

$$\theta = 180 - \alpha/2 \qquad (3)$$

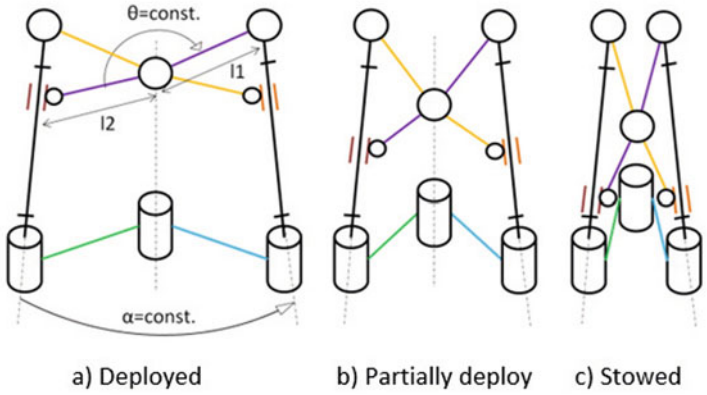

Figure 2 Sarrus-Pantograph linkage schematic diagram

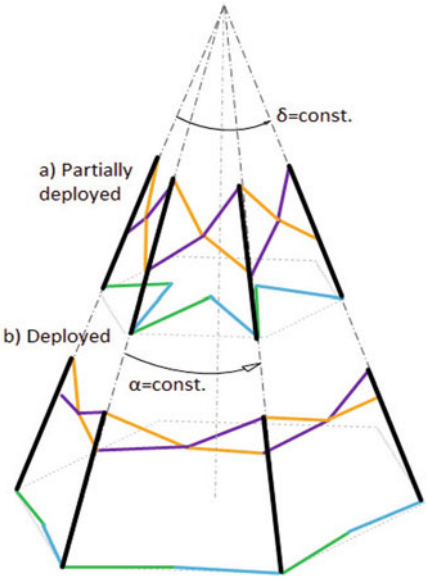

Figure 3 Sarrus-Pantograph hexagonal ring constant cone angle δ and α schematic

The concept presented above was successfully developed into a TRL3 demonstrator which to date has undergone more than 50 deployments under a 1g environment without a single failure. The physical demonstrator is depicted in Figure 4. Although the mobility criteria presented above reveals that the mechanism can be actuated from a single point, three actuation mechanisms are present in the structure to avoid single point failures and to evenly distribute deployment forces in the structural elements. Stored energy elements are strategically position in the mechanism to achieve its "blooming" immediately after the hold down and release mechanism is actuated. This allows a transition of the mechanism from a fully stowed geometry to a more advantageous configuration before motorized actuation kicks-in and realizes full deployment of the motion structure.

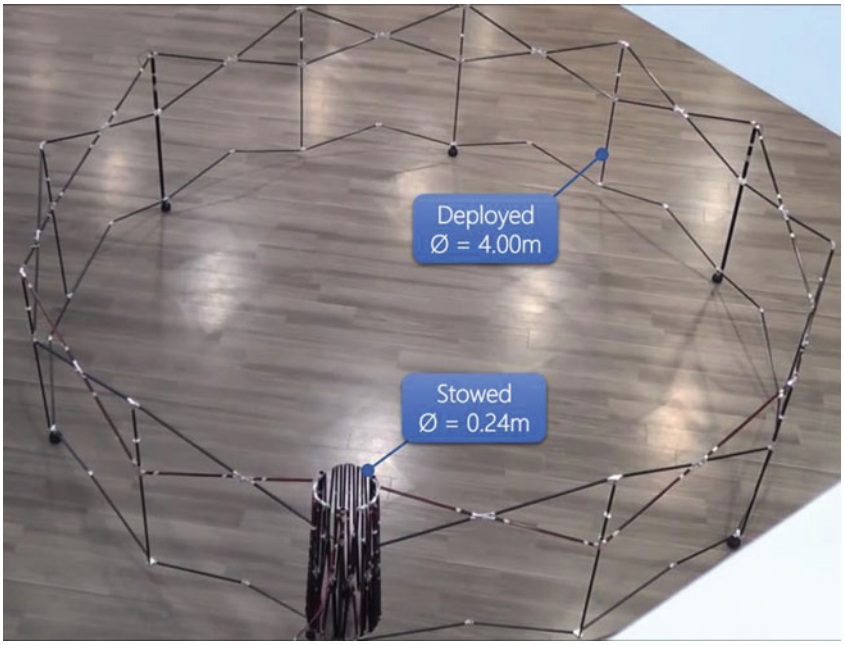

Figure 4 TRL3 demonstrator of the Sarrus-Pantograph RDS in its stowed and fully deployed configurations

Table 1 shows the budgets measured on the TRL3 demonstrator. The deployed diameter shown is the average diameter measure from 5 deployments.

Table 1: Main RDS budgets

Budget	Dimension measured or (estimated)	Margin	Dimension including margin
LDA Structure (incl. actuators) mass	7.0 kg	-	7.0 kg
4m Shell-membrane	(6.300 kg)	20%	7.560 kg
Total mass	**-**	**-**	**14.56 kg**
Deployed top diameter	3.953 m	-	3.953 m
Stowed top diameter	0.23 m	-	0.23 m
Stowed bottom diameter	0.33 m	-	0.33 m
Stowed internal diameter	0.18 m	-	0.18 m
Height	1.07 m	-	1.07 m
Deployment time	321 s	-	321 s

The power budget is a critical requirement that needs close monitoring and which limits the type and number of actuation points in all motion structures. Power demand during deployment in a 1 g environment was monitored during three deployment tests. The current was recorded for each actuator (unit 1, 2 and 3) every 10s during the said deployments and the calculated power was plotted against time in Figure 5.

The actuator power appears consistent over the 3 deployment events. Unit 2 power consumption (in red) is slightly higher than unit 1 (in blue) and 3 (in green); nevertheless all follow the same profile. The total power for each deployment (in orange, sum of 3 units) shows consistency. The maximum total power recorded was 8.40W. The thick light blue line on Fig 4 is the average total power over the 3 deployments.

The TRL3 demonstrator and the trade-off studies conducted to date show the proposed architecture offers a promising novel RDS which should serve as the foundation in future flight programmes.

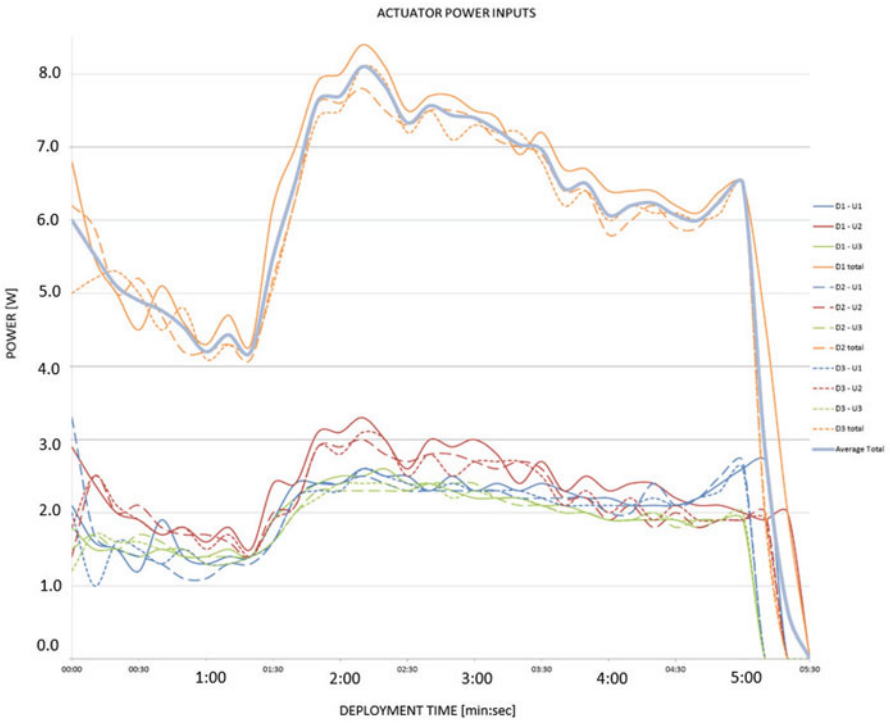

Figure 5 Power demand monitored in each actuator of the OSS RDS

Reflector Surface Technology Status

To meet the forecast emergence in demand and growth of a large market for high frequency (X- to Ka-band) deployable antenna reflectors over the coming decade, OSS are developing the necessary subcomponents to deliver such a product, including antenna deployment boom (currently at TRL6, part funded through InnovateUK), deployable reflector dish outer ring structure (currently at TRL3 as described in the previous section, funded through ESA) and the flexible reflector surface itself. This section highlights the initial research conducted by OSS into flexible reflector surface materials and gives an indication of planned future work, part funded through NATEP.

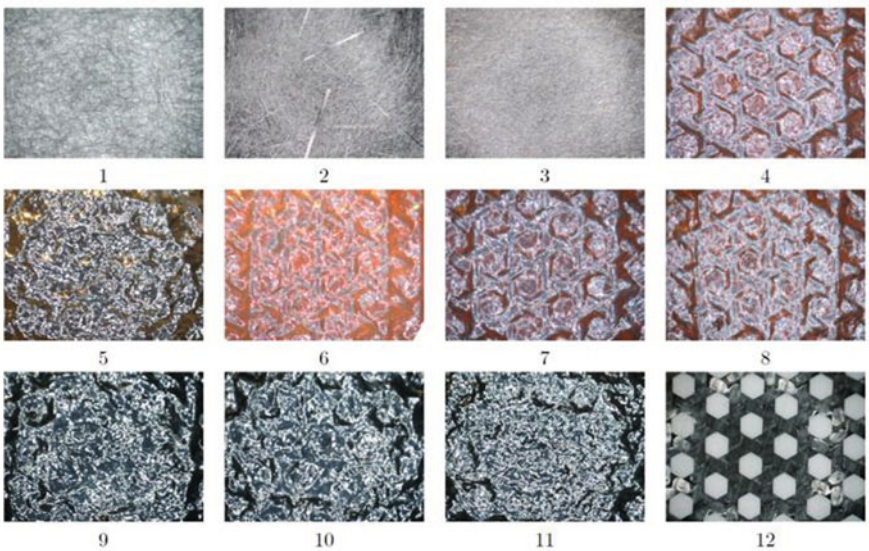

Figure 6 All 12 reflector surface materials tested. Each sample is composed from a unique combination of space compatible carbon fibre structures, silicone compounds, and metallic nanoparticle materials.

Reflector Surface RF Studies

All measurements on the 12 reflector surface material coupons in Figure 6 were obtained at ambient temperature with a Rohde&Schwarz ZVA-40 Vector Network Analyser (VNA). For the free space measurements, the samples were held at the aperture of a Ka-band corrugated feed horn. For that purpose they were placed on a 10mm thick sheet of low density Styrofoam which was in direct contact with the feed aperture. The reflections were determined by a S11 measurement at the waveguide port of the feed. An additional open ended waveguide probe was placed at a distance of 0.4m above the feed for simultaneous S21 measurements which were used to determine the transmission through the samples. The measurements were calibrated with a flat Aluminium plate reflector in the same setup as the samples under test.

The mismatch of the feed and the waveguide transition was determined by a free space absorber between the feed and waveguide probe acting as a matched load standard. Figure 7(a) shows this free space measurement setup without the supporting Styrofoam sheet. Though effective for lossy samples, the highly reflective samples under test and the reference reflector the S11 results are affected by sharp resonant features. These are caused by higher order modes that are trapped in the high-Q cavity which is formed by the feed horn and the sample. In order to mitigate this problem, the data was recorded with high frequency resolution (i.e. 5MHz for the 22–40GHz range or 3600 points), and only data points outside of the resonances were taken into account. The results were further binned using the median value to reduce the impact of outliers.

An alternative approach would be time gating of the signal in the VNA. The results of the freespace measurements depend significantly on the alignment and flatness of the samples. Because of this, it was difficult to determine the reflectivity with a resolution better than 0.1dB with the setup used.

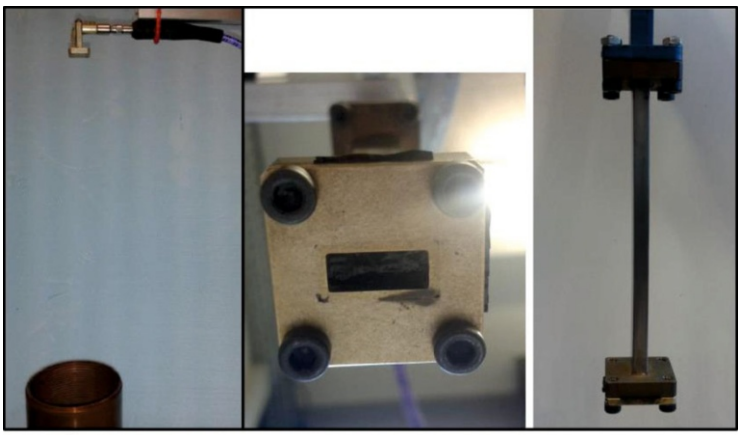

Figure 7 Test setup for ambient (a.) freespace and (b.) waveguide RF testing

In addition to the free space measurements, the reflectivity was also measured by S11 measurements: where the samples were placed in direct contact with an open ended waveguide port. The data of this test series was calibrated by a full 1-port calibration of the VNA using a matched load and two offset shorts for WR-28. Since the waveguide is singlemoded, the measurements are not degraded by any sharp resonances. However, this geometry is not fully representative for the free-space performance of the samples.

The results depend significantly on the physical contact between the sample and the waveguide interface. The isolating silicone layer at the surface of the composite will lead to a lateral power leakage at the waveguide flange. It appears as an apparent loss in this test, which would not be present in a free space setup. For this reason, the setup has overestimated the losses.

The dimensions of the waveguide are not much larger than the scale length of woven carbon fabric, meaning the S11 results should depend on the alignment between fabric and waveguide. This effect should be most pronounced for plain woven carbon sample #12. The measurements of sample #12 were repeated four times with different

systematic alignments, resulting in differences up to 0.2dB. However, it was quite apparent that for samples #1 - #11 this variation is greatly suppressed due to an inherently different configuration of composite.

Given the uncertainties of both methods, the reflectivity results with the free space and waveguide setup are in reasonably good agreement with each other. On average, measurements of reflection efficiency using the two methodologies varied by 0.02dB / 0.5%.

In terms of reflection efficiency, sample #4 presented the most promising results. Not only had it achieved the highest reflection efficiency, averaging approximately -0.27dB / 94%, it demonstrated relatively high consistency in reflection efficiency over the full Ka-band spectrum, unlike say sample #12 that dropped in performance by approximately 0.4dB / 7% at 40 GHz compared to performance at 26.5 GHz. A great deal of this loss can be attributed with the relatively open weave of the structure. At higher frequencies, more Ka-band waves simply pass through these open apertures within the reflector surface. On average, 5.9% of waves directed at #12 simply pass through. Samples #1 - #11, however, have an additional component within the composite to reduce this particular form of transmission loss. This component is quite successful, reducing losses to between 0.0014 and 0.0389%, and increasing consistency of reflection efficiency through the full sweep of Ka-band.

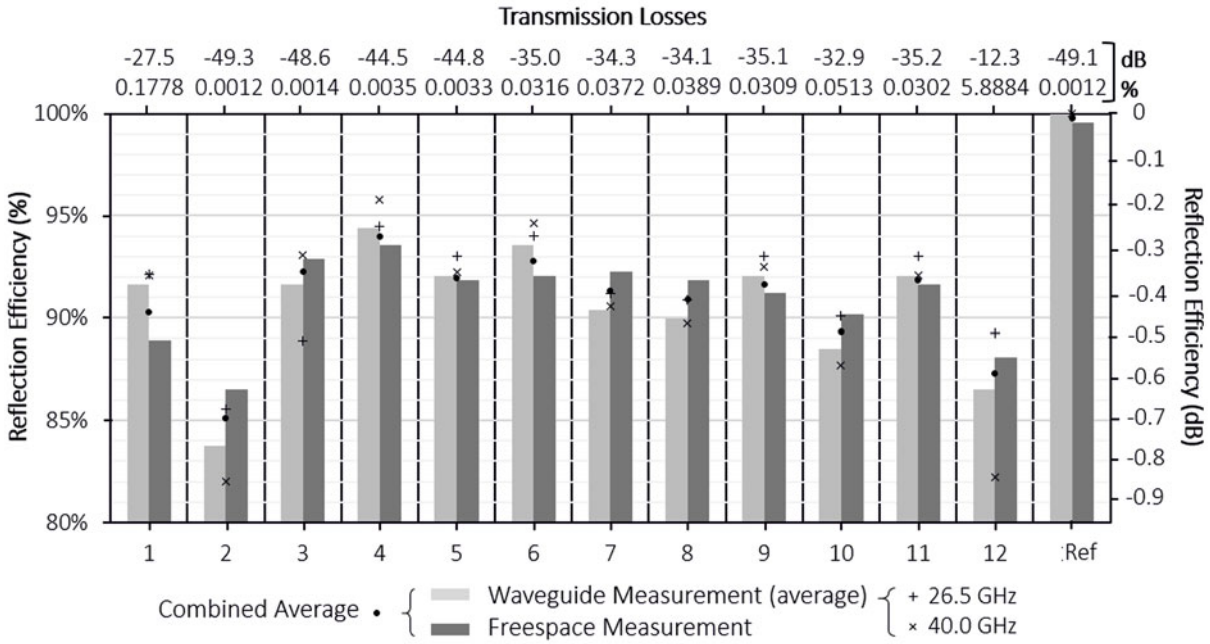

Figure 8 Summary of results for ambient reflection efficiency and transmission losses of the 12 reflector surface materials selected and developed compared to a reference aluminium plate

Considering sample #12 represents the current state-of-the-art in high frequency flexible carbon reflector surfaces globally, at least for this initial stage of RF testing, OSS seems to have formulated a more competitive solution – deeming further exploration of sample #4 at least. Compared to the performance of the AstroMesh 30 OPI metal mesh, the best commercially available flexible reflector surface considered usable for high frequency applications, sample #4 is comparable. Reflection efficiency for sample #4 at 26.5 GHz is -0.25dB / 94.5% and at 40 GHz is -0.19 dB / 95.8%. Reflection efficiency of the metal mesh at 26.5 GHz is -0.17dB / 96% and at 40 GHz is -0.36 dB / 92% . However, at the dish level, there can be expected to be additional complications inherently in the design of a metal mesh reflector that would further reduced reflection efficiency and overall system competitiveness compared to a moulded carbon fibre based reflector. These including pillowing, significant pre-tensioning, and thermal distortions. Quantification of the magnitude of the advantage a moulded carbon fibre based solution would have over a metal mesh solution in this sense is yet to be determined.

Reflector Surface Mechanical Studies

A significant mechanical aspect of the flexible reflector surface material developed is its minimum bend radius. This radius determines how tightly the material can be folded before the onset of damage within the material occurs. Damage to the reflector surface material will vary the mechanical properties in an uncontrolled way and will lead to plastic geometric distortions. These two variables inherently reduce the RMS accuracy achievable at the reflector dish level. Finding the minimum bend radius of the material developed by OSS will allow this constraint to be incorporated into the stowage technique adopted, if a practical one exists.

A Platen-type test was conducted with sample #4 to find approximately at what point damage occurred over a range of bend radii. This damage was determined on visual inspection using a CT scanner. Each coupon was CT scanned before testing to determine whether or not the material was already damaged, they were then bent to a given radii (between 10mm – 1mm), see Figure 9, and were finally CT scanned again to determine if any damage had occurred (and the nature of that damage). When CT scanning, each coupon was imaged at 6 equally spaced regions through-thickness, see Figure 10(a-c), and was inspected. An example of damage found through creasing is highlighted, see Fig 10(d).

Though far from conclusive, the onset of damage begins to appear at a bend radii of approximately 3mm. Damage was never more than very small, low in distribution and size, affecting never more than ~1% of the fibres bundles inspected. Though some coupons were bent to 1mm radius without damage, other coupons began showing damage at approximately 3mm. The conclusion from this testing was that the reflector surface material developed has a very small minimum bend radius, well within the requirements for the practical stowage of a flexible parabolic reflector.

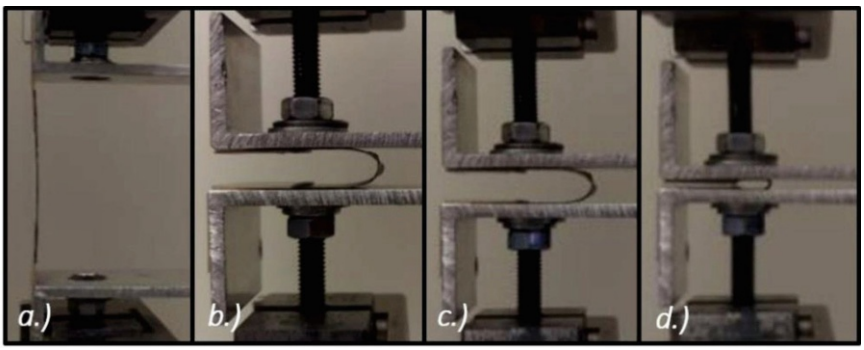

Figure 9 Platen-type testing using position controlled Instron, reducing bend radii of individual coupons of sample #4 from a.) ∞ to b.) 3.75mm, c.) 2.5mm, d.) 1mm.

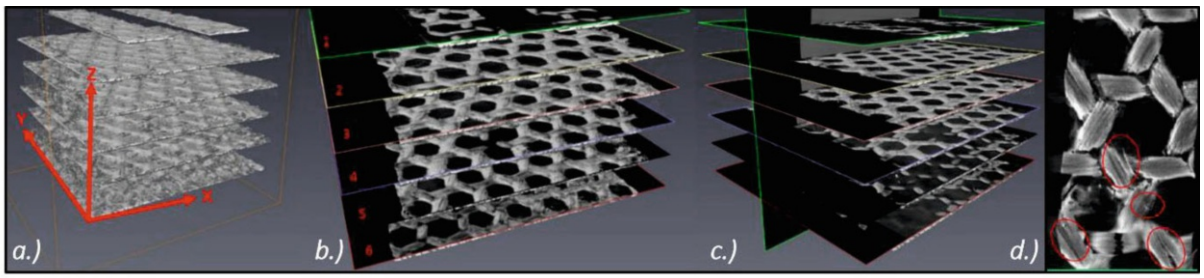

Figure 10 CT scan layers, a.) orientation of planes, b.) through-thickness slices of sample, c.) XZ and XY planes, d.) example of damage to material caused through a hard crease

Reflector Surface Folding Studies

Folding techniques for the parabolic reflector dish are being explored using FE simulations and the mechanical properties garnered thus far from sample #4. This line of study is being used to minimise the stowage volume of the folded reflector surface without causing damage to the material.

Creases in the material would reduce the level of control in the deployed shape of the reflector surface due to localised variation in mechanical properties and plastic geometric distortions. These introduced variables would subsequently reduce the RMS accuracy of the deployed shape achieved. This contribution to a reduction in RMS surface accuracy would reduce the frequency at which the structure is deemed capable of operation.

Creases, and the associated onset of damage, are determined by the minimum bend radius of the reflector surface material. FE studies allow for folding techniques to be explored whilst stresses, strains, and bend radii are relatively easily monitored. Non-linear FE techniques have been applied to model the mechanical and kinematic behaviour of the flexible reflector surface, this is an on-going study and conclusive results will be presented in a subsequent paper. Some membrane deployment simulation results are presented in Figure 11.

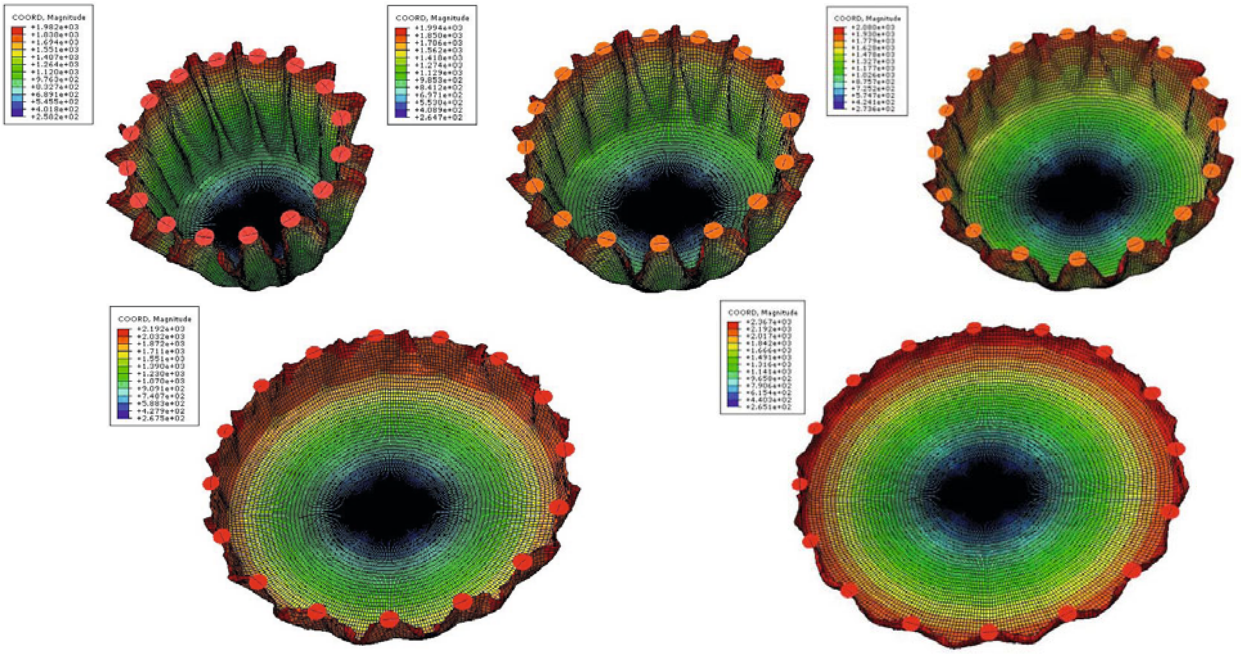

Figure 11 Finite Element analysis of the reflector surface deployment sequence

FUTURE WORK

OSS are in the process of conducting thermal tests on the reflector surface material at the composite and sub-component level in order to develop a deeper understanding of the thermal properties of the surface material, with particular focus on its thermal expansion coefficient and profile. This information will feed into FE studies to help indicate the geometric shape accuracy capabilities of the material, in terms of root-mean square (RMS) accuracy, at the reflector dish level and in the space environment.

OSS and project partners are currently at the detailed design level in the development of a generic deployment rig for a full-scale parabolic dish breadboard of the reflector surface material and support structure. A stiff and generic rig has been decided upon to test the deployment and deployed RMS accuracy of a range of deployable reflector surfaces (≤5m diameter) independent from the induced errors associated with the rest of a flight-worthy RDS. This mechanism and testing will not only allow for the validation of FE studies, it will enable iterative optimisation of the reflector surface material and support structure configuration through this coupled FE analysis and experimentation to maximise RMS accuracy. The generic deployment rig is expected to be operational by early Q2 2016.

Transition from coupon level to full-scale parabolic dish of the reflector surface composite material in terms of manufacturing technique is a significant challenge particularly when considering the geometric tolerances necessary

for RF operations at Ka-band; <0.25mm RMS accuracy. Manufacturing techniques of such complex membrane structures will be the focus of subsequent papers.

ACKNOWLEDGEMENTS

OSS would like to thank ESA for their financial and technical support in the development of the RDS TRL3 demonstrator, the UK National Aerospace Technology Exploitation Programme (NATEP) for part-funding this research; without their backing, the research into foldable reflector materials would not have been conducted. OSS would also like to thank Dr Axel Murk from IAP Bern for conducting the RF testing presented in this paper the team under Prof. Michele Meo at the University of Bath carrying out the mechanical testing and inspection on the reflector surface material shown here.

REFERENCES

1. Mangenot, C., Saniago-Prowald, J, Van T'Klooster, K, et al (2010). Large Reflector Antenna Working Group - Final Report, ESTEC, 8 September 2010.

2. Magliorelli, L., Scialino, L., Breunig, E. *et al* (2011). Reflector Technology Trade-off for LDA on Telecom and Earth Observation Applications, *Proceedings of the 33rd ESA antenna workshop on challenges for space antenna systems.,* ESTEC Noordwijk, The Netherlands, 18-21 October 2011.

3. Z. You & Y. Chen (2012). Planar double chain linkages. In: *Motion Structure. Deployable Structural Assemblies of Mechanisms.* Spon Press 2012.

4. V. Fraux, J. R. Reveles, M. Lawton, Z. You, Novel Large Deployable Antenna Backing Structure Concepts for Foldable Reflectors, *CEAS Space Journal,* Vol. 5, Issue 3-4, pp 195-201, (2013).

5. V. Fraux, J.R. Reveles, M. Lawton, Novel Large Deployable Antenna Backing Structure Test Campaign, *Proceedings of the 2nd International Conference in Advanced Lightweight Structures and Reflector Antennas*, 1-3 October 2014, Tbilisi Georgia.

6. J. Santiago Prowald & M. Such Taboada. Innovative Deployable Reflector Design, *Proceedings of the 33rd ESA antenna workshop on challenges for space antenna systems.,* ESTEC Noordwijk, The Netherlands, 18-21 October 2011.